Route to hyperchaos in a system of coupled oscillators with multistability

N. J. McCullen* and P. Moresco
School of Physics and Astronomy, University of Manchester, United Kingdom
(Received 5 October 2010; published 19 April 2011)

This work presents the results of a detailed experimental study into the transition between synchronized, low-dimensional, and unsynchronized, high-dimensional dynamics using a system of coupled electronic chaotic oscillators. Novel data analysis techniques have been employed to reveal that a hyperchaotic attractor can arise from the amalgamation of two nonattracting sets. These originate from initially multistable low-dimensional attractors which experience a smooth transition from low- to high-dimensional chaotic behavior, losing stability through a bubbling bifurcation. Numerical techniques were also employed to verify and expand on the experimental results, giving evidence on the locally unstable invariant sets contained within the globally stable hyperchaotic attractor. This particular route to hyperchaos also results in the possibility of phenomena (such as unstable dimension variability) that can be a major obstruction to shadowing and predictability in chaotic systems.

DOI: 10.1103/PhysRevE.83.046212 PACS number(s): 05.45.Tp, 05.45.Gg

I. INTRODUCTION

Simple nonlinear systems can give rise to highly complicated or chaotic dynamics, whereby long-term prediction is practically impossible. When such systems are coupled to form higher dimensional systems, there may seem to be little hope of accurately modeling the dynamics of the system as a whole. However, under certain conditions, degrees of predictability can exist and it may therefore prove possible to model a variety of complex natural phenomena. Much is known theoretically about low-dimensional chaos and trajectories of some models can be proven to stay close to, or *shadow*, the dynamics of the real physical system [1]. Synchronization of coupled chaotic oscillators is also possible [2], leading to the system exhibiting lower dimensional dynamics than would otherwise be observed.

Thus an important problem in nonlinear physics is that of trying to understand the conditions under which the dynamical variables are confined to low-dimensional behavior in the full phase space of the system. The hope is that systems with multiple interacting components may exhibit lower dimensional dynamics through synchronization and therefore be less unpredictable in their behavior. This is important when trying to model complex natural systems such as the climate or weather. In numerical weather prediction synchronization is also used to entrain model trajectories to observation data in order to more accurately forecast the future behavior of the true system [3,4]. Results are presented here of an experimental investigation on a system of coupled electronic oscillators. The system is studied using novel data-analysis techniques to reveal a stable hyperchaotic state arising from the interaction of two hyperchaotic nonattracting sets, which originate from two phase-multistable synchronization states. The subsets of the attractor are found to lose individual stability when they become hyperchaotic through bifurcations of the unstable periodic orbits they contain—a case of attractor bubbling. While this mechanism to create a hyperchaotic set may not be generic, it is believed to be one important route to hyperchaos. In the following sections we describe the phenomena of interest and introduce the methods and physical system used to demonstrate the transition from low-dimensional chaos to *hyperchaos*, which is potentially *unshadowable*. This experimental study draws on various theoretical concepts and provides evidence for links between phenomena such as synchronization, attractor bubbling, and phase multistability, as well as interacting invariant sets and *unstable dimension variability*, the latter a major obstruction to predictability through shadowing.

A. Synchronization of chaotic signals

Although chaotic systems exhibit sensitivity to initial conditions, various degrees of synchronization between them is also possible. Systems exhibiting chaotic oscillations can become synchronized when the frequencies of oscillation of their variables become entrained and their relative phases bounded. For coupled and high-dimensional systems, the transition from low to high-dimensional dynamics is often associated with the loss of synchronization between the system. There are several classes of chaos synchronization, each representing a different degree to which the systems lose their independence with respect to each other.

Complete synchronization (CS) of chaotic signals is the perfect synchronization of interacting systems, where the instantaneous states of the systems are identically matched [5,6]. Attractors of a chaotic system contain a dense set of unstable periodic orbits (UPOs) and synchronization in this case comes about when the respective UPOs of the subsystems become locked, in a similar manner to phase locking in stable limit cycles. A difference in the natural frequencies of the subsystems results in a phase difference appearing, known as *phase synchronization* [7,8].

A weaker type of synchronization between interacting chaotic systems is where there is not an exact match between the amplitudes of subsystems but there still exists some (often complicated) functional relationship which maps states from one subsystem onto the next:

$$x_2 = g(x_1). \tag{1}$$

*Present address: School of Applied Mathematics, University of Leeds, UK.; N.McCullen@physics.org

This *generalized synchronization* (GS) implies a one-to-one equivalence between states in the subsystems [9]. This implies that the two subsystems are not independent and there still exists a synchronization manifold to which the dynamics are restricted. Also, in discretizations of spatiotemporal systems this form of synchronization is important for spatial structures such as waves and patterns to exist. The degree of GS is also related to the number of positive Lyapunov exponents in the system, with its onset characterized by a positive Lyapunov exponent crossing zero [10]. This type of synchronization is utilized in current attempts to forecast the weather using data assimilation [3,4]. The loss of GS can occur when the UPOs contained within the attractors bifurcate and become unstable transverse to the synchronization manifold [11] and correlations between amplitudes cannot be detected. The case where there is only period entrainment and phase locking but no correlations in amplitude is known as *phase synchronization*, and *imperfect phase synchronization* when phase slips occur. Systems which are phase synchronized can be entrained in configurations where they are either in phase or out of phase [12]. In certain cases both these states can co-exist, a phenomenon known as *phase multistability* [13]. In the current system we find phase multistable behavior, as described in more detail in Sec. II D, and this proves crucial to understanding the transition between synchronized and hyperchaotic dynamics.

B. Shadowing breakdown in hyperchaotic systems

The set of UPOs in chaotic attractors results in typical trajectories possessing, on average, an unstable (expanding) direction to the flow in phase-space, corresponding to a positive Lyapunov exponent. Despite this, under the specific conditions of *hyperbolicity* the motion is said to be *shadowable*, whereby there can be proven to exist trajectories in the physical system which lie close to (*shadow*) numerically computed *pseudotrajectories* for an arbitrary length of time, known as the *shadowing time* [1]. In these cases there is hope that we can accurately model nature and provide a degree of reasonable prediction. However, in dissipative systems with more than three degrees of freedom there can be more than one locally expanding direction to the flow, where trajectories have multiple positive Lyapunov exponents. Here, attractors can suffer from phenomena which render a system *unshadowable*, rendering model predictions unreliable [1,14–20]. In hyperchaotic attractors a phenomenon known as *unstable dimension variability* (UDV) is believed to be commonplace [20], whereby there are variations in the dimension of the expanding and contracting subspaces in different parts of the set along a typical trajectory. In this case the obstruction to shadowing is especially severe and computed averages are highly unreliable in such cases [21–26]. This phenomenon has previously been studied in the current system [27], and the current work sheds light on the origins of that state.

It is important to understand the origin of hyperchaos and nonhyperbolicities in systems capable of obtaining more than one positive Lyapunov exponent. This will help in understanding the structure of hyperchaotic attractors, which is currently not very well known. It has been previously shown theoretically how hyperchaotic attractors containing UPOs with different numbers of unstable directions can be formed by the interaction with nonattracting sets inside the attractor [28]. The following results show experimentally that a hyperchaotic attractor is formed here in a similar manner, as two nonattracting, individually unstable sets merge. This can be seen as analogous to the way that chaotic attractors contain a set of unstable periodic orbits. The transition to hyperchaos is shown to be due to bifurcations of the UPOs contained within each set in the direction transverse to a direction of stability; an experimental demonstration of attractor bubbling. It has also been shown theoretically and numerically how the smooth transition to hyperchaos via bifurcations of the UPOs is intrinsically linked to the existence of UDV in the system [29,30]. This is also observed here experimentally and presented in Sec. III.

C. Method for determining the unstable dimension

The techniques described herein work on attractors reconstructed from a single dynamical variable using embedding techniques based on Takens' theorem [31]. From this, quantities such as Lyapunov exponents and the topological dimension measures used in this work can be estimated. Lyapunov exponents quantify the rate of exponential expansion or contraction of volumes over the whole of a given attractor and thus characterize the expanding (unstable) and contracting (stable) directions in phase-space. However, the presence of noise and constraints in the amount of data available impose serious limitations on techniques available for calculation of Lyapunov exponents from experimental data [32]; this is a particular problem when trying to obtain short time Lyapunov exponents (STLEs), which give information on the local rather than global expansion and contraction rates.

Here we use a method for measuring the expanding subspace of attractors reconstructed from experimental data that does not require the calculation of STLEs. The method determines the topological dimension of the unstable space for points along a trajectory on the attractor using geometric arguments. The technique, described in detail in our earlier work [27], builds on ideas in work by Hammersley [33] and, later, Bennet [34]. Hammersley showed mathematically how the mean interpoint distance between pairs of points in hyperspheres increases with the dimension of the hypersphere in which they are embedded. Hammersley's analysis was for homogeneously distributed points but the principle works well for less uniformly distributed data also. Bennet used this result to investigate the dimensionality of signals, producing numerical values from Hammersley's formulas. These values relate this mean distance between points in phase space and the dimension of the signal. The calculated mean interpoint distances for sets of points in one, two, and three dimensions is 0.333, 0.453, and 0.514, respectively. Our method first looks at points belonging to numerous trajectories within a fixed radius of a point of interest on the attractor and calculates mean interpoint distance between all pairs of points in the set, which is directly related to the local topological dimension in the manner stated above. This dimension is always equal to the number of expanding (unstable) directions plus the neutral direction of the flow, along which points neither expand nor contract. This process is repeated, using many sites on

the attractor as origins for the hyperspheres containing the trajectory points used in the calculations. Therefore if we plot histograms of these local dimension measurements for many locations on the attractor it is possible to infer the degree to which the variables are synchronized and determine the number of unstable dimensions and whether this is fixed along a typical trajectory. This is subsequently referred to as the interpoint distance (IPD) method.

II. RESULTS FROM A SYSTEM OF COUPLED OSCILLATORS

A. Experimental system

Electronic oscillators were used for this study due to the high degree of control over the parameters of the system and the large amounts of high quality data that can be quickly obtained. Any mismatch of parameters and the small effects of noise are from real sources and therefore closer to real-world systems. The individual oscillator units are based on a modification of the van der Pol oscillator circuit [35], utilizing solid state components [27,36,37], with data obtained by measuring the potential difference between two points in the circuit and measured at a high sampling rate.

Each oscillator has three degrees of freedom and is capable of exhibiting chaotic behavior. When oscillators are coupled together the resulting systems can exhibit higher dimensional dynamics, such as various degrees of synchronization and hyperchaos. The coupling links make use of high impedance op-amps, allowing the signal to be fed from one point in the coupled circuit to another without any feedback [37]. The coupling strength can also be adjusted, providing a further control parameter.

B. Model system

An oscillator O_i, which experiences a coupled signal from another oscillator O_j, can be represented using the following set of equations:

$$\begin{aligned} \dot{x}_i &= \mu\left[\frac{(y_i - x_i)}{\beta_i} + f(y_i - x_i) - \alpha_0 + \alpha_i(x_i - \sigma x_j)\right], \\ \dot{y}_i &= -z_i - \frac{(y_i - x_i)}{\beta_i} - f(y_i - x_i), \\ \dot{z}_i &= y_i - \rho z_i, \end{aligned} \tag{2}$$

where x_i, y_i, and z_i are dimensionless voltages and currents at various points in the circuit of the ith oscillator, β_i is a nondimensionalization of the variable parameter and α_i of the negative resistance in the circuit. The function $f(V)$ is the voltage response of the nonlinear element, which in its full form is the exponential $f(V) = I_p(e^{k(V)} - e^{-k(V)})$, but can be well represented by a series expansion up to cubic order in V [36]. The overdot represents differentiation with respect to nondimensional time τ. The parameter σ is the strength of coupling between elements, experimentally controlled by a variable resistor, and all other symbols are dimensionless scaling constants, obtained by measurement of elements in the circuit [37]. The values for the constants, used in numerical simulations to confirm the physical observations, were approximately $\mu = 3.9$, $I_p = 1.87 \times 10^{-6}$, $k = 3.9$, and $\rho = 0.042$. For the current investigation the individual oscillators were carefully balanced with respect to each other in order to prevent detuning and other imperfections from breaking the synchronization. In terms of the parameters this means that $\beta_1 \approx \beta_2 \equiv \beta$ and $\alpha_1 \approx \alpha_2 \equiv \alpha(\approx \frac{1}{3})$. The small but inevitable imperfections in the system are modeled by a simple linear term $\alpha_0 = 7.2 \times 10^{-3}$ in Eq. (2) [38]. Only a single variable x_i for each oscillator was measured, with the system reconstructed using the time-series delay embedding techniques derived from Takens' theorem [31]. This has the dual advantage of of both making the techniques more readily applicable to physical systems where not all of the variables are accessible and also simplifying the following analysis.

C. Behavior of the coupled system

In isolation each subsystem has a pair of solutions, which originate in the $x < 0$ and $x > 0$ branches of a pitchfork bifurcation from a null equilibrium solution. On increasing the bifurcation parameter β, the system bifurcates from the nonzero fixed point via a Hopf bifurcation and a sequence of period doublings resulting in chaos. At higher values of β the degenerate attractors in the negative and positive voltage regimes combine to form one large double-lobed "glued" state [39]. The imperfections in the system, modeled by the α_0 term in Eqs. (2) are assumed to be a constant offset in the operational amplifier. The effect of this offset is to disconnect the branches of the pitchfork bifurcation, breaking the reflection symmetry of the subsequent dynamics and shifting the various bifurcations to different parameter values on each branch. The coupled signal from O_i introduces a perturbation (proportional to x_i) to the α_0 term of the O_j, shifting its bifurcations accordingly. This mutual addition to the imperfection term of each oscillator disconnects the branch corresponding to the voltage state of the other. Furthermore, at the parameter values used here, where $x_{1,2}$ have large magnitudes, the disconnected branch of the pitchfork bifurcation is shifted to parameter values out of the range of the current study, forcing states on the continuous branches of each oscillator to always have the opposite sign.

D. Synchronization sets and phase multistability

For certain parameter values, the oscillators are found to be synchronized, but not identically. The focus of oscillation of each of the x variables for both oscillators, $\bar{x_1}$ and $\bar{x_2}$, are related by a sign change such that $\bar{x_1} = -\bar{x_2}$. The dynamics of the individual oscillators can synchronize in two ways in this regime, one with the phases locked with the amplitudes in perfect antiphase about the origin, and the other with both a sign change and a π phase shift. This results in two distinct states of the system, which coexist multistably. These states can be seen in Fig. 1. Both in-phase and antiphase oscillations have been observed in a range of systems [12,13,40]. This form of phase degeneracy was shown in [13] to be important in understanding the transition to hyperchaos.

At parameter values just above the Hopf bifurcation the oscillations are almost sinusoidal and symmetric under the transformation $[t \to t + T/2, (x - x_0) \to -(x - x_0)]$, where T is the period and x_0 is the focus of oscillation. However, at

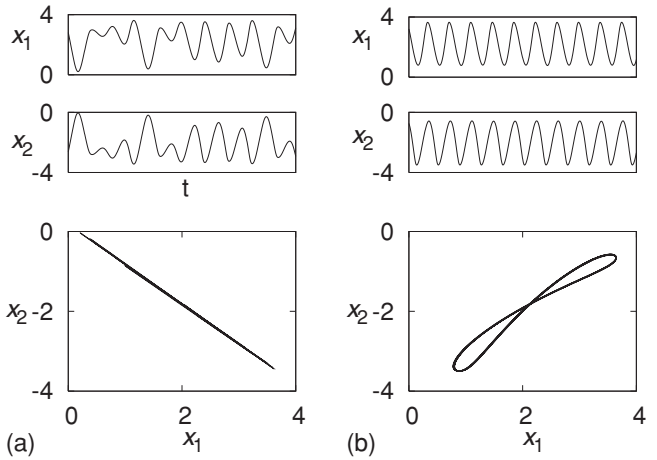

FIG. 1. Time-series and phase portraits showing the phase multistable states. At low β the oscillators can lock in two states. In (a) oscillations are antisymmetrically synchronized (AS) whereas in (b) they are synchronized with an additional phase lag. The characteristic states of regions "A" and "B" in Fig. 2 are of the type shown here in (a) and (b), respectively. The oscillations of AS exhibit perfectly synchronized chaos (of opposite sign) at the same value of β where the lag-symmetric (LS) states which dominate in region "B" are limit cycles.

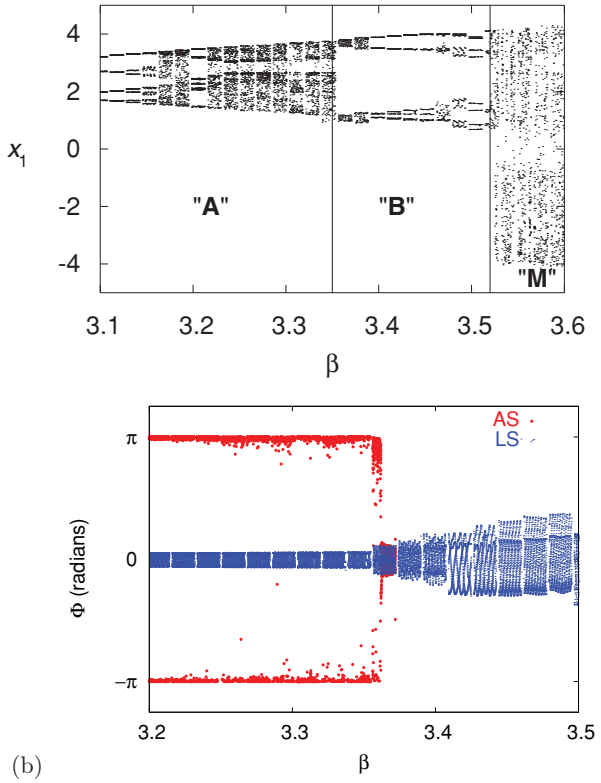

FIG. 2. (Color online) Experimental bifurcation diagram for the two-in-a-ring system (a), showing the transition when starting from the antisymmetric state AS. Oscillations bifurcate to chaos in region "A" before returning to periodic lag-symmetric LS states in region "B." These then bifurcate to chaos again before a third, mixed state is encountered in "M," which is found to be hyperchaotic. (b) Bifurcation diagram based on the difference in the phases $\Phi = \phi_1 - \phi_2$ is shown at various β in the bifurcation diagram. Both the phase-symmetric ($\Phi = 0$) AS state and the π phase-shifted LS state coexist for values of $\beta \lesssim 3.35$. The AS state (red circles) loses stability to the LS state (blue dots) as β is increased. When LS also loses stability the mixture of the two unstable saddles, the remnants of the AS and LS attractors, forms the globally stable hyperchaotic attractor. Numerical computations show almost identical behavior, with small differences in the exact parameter values due to the tiny mismatch between the numerical and inexactly known experimental values.

higher parameter values the oscillations are asymmetric and contain higher harmonics and $x_n(t) \neq -x_n(t + T/2)$. In these cases there is a mirror symmetry about the time axis between the states of the two oscillators, such that $x_1(t) = -x_2(t)$ for one state and $x_1(t) = -x_2(t + T/2)$ for the other. These properties can be seen in Figs. 1(a) and 1(b) at the same value of β. The phase relationship shown in (a), where $x_1(t) = -x_2(t)$, will be referred to as the *antisymmetric* AS state and those states having the phase relationship shown in (b), where $x_1(t) = -x_2(t + T/2)$, as *lag symmetric* (LS). The one parameter bifurcation diagram for the region of interest is shown in Fig. 2(a), obtained by varying the combined parameter β and recording the variable x_1.

The dynamics here can be divided into three regions, characterized by the different mix of dynamical behaviors encountered within them. In the region labeled "A" the AS oscillations are preferred by the system and most likely to be encountered from an arbitrary initial condition. The LS states can also be found at these same parameter values, a case of phase multistability. However, in region "B" the AS states are absent and in "M" the phase is found to be a mixture of both types of behavior (later shown to be an amalgamation of the nonattracting remnants of both sets).

It is observed that bifurcations of AS and LS are found to occur at different parameter values; notably, LS states are limit cycle until after AS has bifurcated to chaos. On a single sweep of the parameter β, starting from an AS state, after the system bifurcates to chaos in AS it loses stability to simple periodic motion in LS at $\beta \approx 3.35$. Shortly after this another sequence of bifurcations follows, resulting again in chaotic motion, this time with LS. At higher parameter values, trajectories enter a mixed state, jumping intermittently between the two phase states, similar to behavior noted in previous numerical studies of phase-multistable systems. In this "M" region, starting at $\beta \approx 3.52$, the system flips between both the negative and positive voltage lobes of a single large attractor, joined by what has previously been identified as a *gluing bifurcation* [39]. The relative phases of the oscillations were obtained from experimental data using the analytic signal method by performing a Hilbert transform on the time series [41]. The bifurcation diagram showing these phases as a function of β is shown in Fig. 2(b). The qualitative dynamics and quantities such as the Lyapunov exponents and stability to perturbations or detuning are therefore different for each of the two states.

Bifurcations of AS and LS were studied experimentally to determine how they separate as the coupling strength is increased and the results are shown in Fig. 3. Here, the loci of Hopf and the first two period doubling bifurcations of both AS and LS are shown in β-σ parameter space. Values at

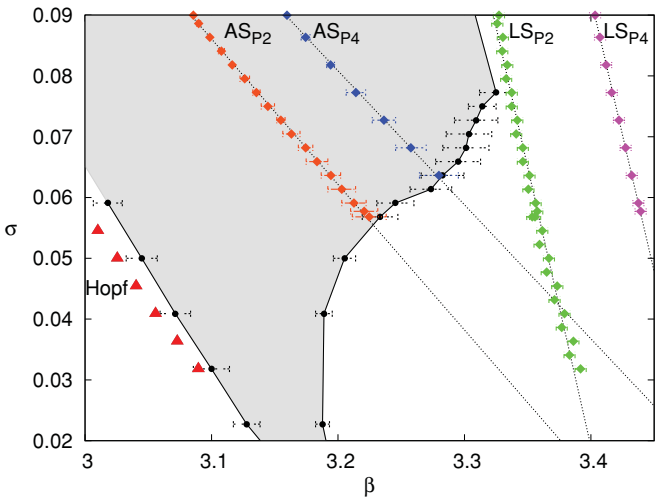

FIG. 3. (Color online) Experimental results showing the shift of bifurcations in β with increasing coupling σ for both AS and LS states. The AS state is stable over less of the parameter space, so parameter values where it appears and then loses stability are shown (AS_{Stab}, black dots joined by lines, surrounding stable shaded region). The loci of Hopf bifurcations are also shown (red triangles), and very slightly above this the states are in perfect synchrony while the amplitude is small and symmetric, before quickly switching to AS when higher harmonics appear. Subscripts P2 and P4 refer to the transition to period-2 and period-4 oscillations, respectively. As before, numerical simulations give qualitatively identical (but parameter shifted) results.

which the AS state first appears and then when it becomes unstable are also shown. Both AS and LS originate from a common Hopf bifurcation, which is offset to lower values of β as σ is increased, due to the coupling dislocating the primary pitchfork bifurcation and resulting in a parameter offset in all subsequent bifurcations. As the coupling strength σ is increased from zero (uncoupled), the two systems interact progressively more strongly, with the various bifurcations shifting in parameter space. However, bifurcations for states synchronized in perfect antiphase (AS) and the lag-symmetric (LS) states are shifted by different amounts. The bifurcations of AS approximately follow the Hopf bifurcation in their relative displacement, but for LS the parameter difference between the Hopf and the first period doubling ($\beta_{P2} - \beta_{Hopf}$) increases on increasing σ. This separates the dynamics of the two phase states in parameter space, with AS bifurcating to chaos at lower values of β than LS.

E. Explanation of the observed stability variation of the phase states

This behavior can be understood using symmetry arguments in the combined system, along with the theorem of Swift [42], as follows. Recalling that the equations of motion have the form

$$\dot{x}_{1/2} = g(x_{1/2}, y_{1/2}) + h(x_{1/2} - \sigma x_{2/1}), \tag{3}$$

where g and h are functions obtained from Eq. (2), the phase difference between the solutions of the two oscillators can now be taken into consideration. Considering only the symmetry in the form of the oscillations and taking the two solutions $x_1(t) = -x_2(t)$ (for AS) and $x_1(t) = -x_2(t + T/2)$ (for LS),

$$\dot{x}_{1/2}(t) = g(x_{1/2}(t), y_{1/2}(t)) + h[(1+\sigma)x_{1/2}(t)] \tag{4}$$

and

$$\dot{x}_{1/2}(t) = g(x_{1/2}(t), y_{1/2}(t)) + h[x_{1/2}(t) + \sigma x_{1/2}(t + T/2)] \tag{5}$$

are obtained for AS and LS, respectively. Now, since $x_1(t)$ and $x_2(t)$ are asymmetric under $[t \to t + T/2, x \to -x]$, it can be seen that the two phase states lead to two unique systems, which diverge more as both σ is increased and the asymmetry of the individual oscillations increases on increasing β beyond the Hopf bifurcation. It is clear from Eq. (4) that, as long as the oscillators are in perfect antiphase synchrony, the coupled system is simply a parameter-shifted version of the single oscillator.

Whereas in AS $x_2(t) = -x_1(t)$, in LS the oscillations are synchronized such that second harmonics are $\frac{\pi}{2}$ out of phase:

$$\begin{aligned} x_1(t) &= Ae^{i\omega_0 t} + Be^{2i\omega_0 t} + C, \\ x_2(t) &= Ae^{i\omega_0 t} - Be^{2i\omega_0 t} - C, \end{aligned} \tag{6}$$

where ω_0 is the frequency of the first harmonic. The second harmonics cancel in the magnitude of the trajectory vector in the phase space of the combined system:

$$|x| \propto e^{i\omega_0 t}, \tag{7}$$

leading to extra symmetry in the system dynamics when compared to oscillations in AS. Swift proved that for a large class of systems period doubling bifurcations are suppressed if symmetry exists in the solutions under the transform $[t \to t + T/2, x \to -x]$, until symmetry breaking occurs [42]. This gives a possible mechanism for the extra stability of LS to bifurcation and chaos.

F. Transition between phase states

The symmetric and asymmetric AS and LS states are stable within a different range of detuning of the individual oscillators, similar to previous work on phase multistability. The work of Postnov *et al.* describes the coexistence of both in-phase and antiphase synchronized attractors in a system, dubbed *phase multistability* [13]. There, phase multistability was found numerically in a coupled Rössler system, with one state losing stability to the other, before they both merged into a single hyperchaotic attractor. Dawson [28] shows how such a stable hyperchaotic set can be formed from invariant nonattracting subsets. The results here demonstrate experimentally the link between these and other phenomena, such as attractor bubbling and UDV, in the origins of the hyperchaotic state.

The Lyapunov exponents of the system were obtained here from experimental data using the method of Wolf *et al.* [43]. The first physical observation of two positive Lyapunov exponents is at the point where AS and LS combine. This is in agreement with the numerical study of Postnov *et al.*, on the coupled Rössler system, where hyperchaos came about as a result of the merger of two phase states [13]. The Lyapunov exponents of AS and LS were also calculated individually using numerical methods. In cases where the

set under investigation was an unstable saddle, the sets were separated using the PIM-simplex method introduced in Ref. [44] and in all numerical cases the Lyapunov exponents were determined using the method of Benettin *et al.* [45]. The results of the application of these methods to AS and LS revealed that the loss of stability of AS coincides with one of the negative Lyapunov exponents crossing zero. Therefore at this point AS becomes a nonattracting set of the system with two expanding (unstable) directions to the flow. A second positive Lyapunov exponent also emerges in LS at the point at which it also becomes a hyperchaotic nonattracting set. However, in this case LS combines with AS to form the mixed state in M, a globally stable hyperchaotic attractor composed of individually non-attracting subsets. This provides evidence that the Lyapunov exponents in M just after the merger come from a combination of those from the individual subsets, due to the fluctuation of trajectories between AS and LS. This is investigated further in Sec. IV using numerical techniques to separate the component sets visited by computed trajectories of the system.

III. LOSS OF SYNCHRONIZATION AND INCREASE IN UNSTABLE DIMENSION

The increase in the dimension of the local unstable manifold (along with the appearance of a second positive Lyapunov exponent) is associated with a reduction in the synchronization between oscillations of the subsystems. In AS the oscillators are initially completely synchronized until the oscillations are well into chaotic regimes. Synchronization then weakens as the system moves toward hyperchaos. A smooth transition to high-dimensional dynamics would suggest a bubbling bifurcation, whereby UPOs in the attractor start to bifurcate and lose stability in the direction transverse to the synchronization manifold [11].

If attractors are indeed experiencing bubbling as orbits deviate from the synchronization manifold when they encounter a transversely bifurcated UPO, this should be detectable by the local dimension of the set of embedded points steadily increasing as this behavior becomes more prominent on increasing β.

The IPD method outlined in Sec. I C was applied over the range of β over which the phase states AS and LS merge. Results are shown in the three-dimensional histogram of Fig. 4. Averaged mean interpoint distances ($\bar{\mu}$) in the reconstructed attractors are shown as histograms in the vertical slices, with the colors indicating the relative occurrences at each value. A smooth transition in the dimension can be seen, from the value associated with a locally two-dimensional manifold [i.e., containing mainly one-dimensional (1D) unstable orbits] toward one with two expanding directions to the flow. This indicates that steadily more of the UPOs contained in the attractor are bifurcating and becoming transversely unstable, thereby displacing trajectories away from the synchronization manifold.

A second peak is seen to emerge in the histograms as the AS state is re-absorbed into the attractor, at around $\beta \approx 3.55$. Two peaks in the histogram indicate that trajectories pass through regions of varying numbers of positive Lyapunov exponents; i.e., the system experiences UDV during the transition to hyperchaos, as predicted previously [29,30]. The peaks for AS

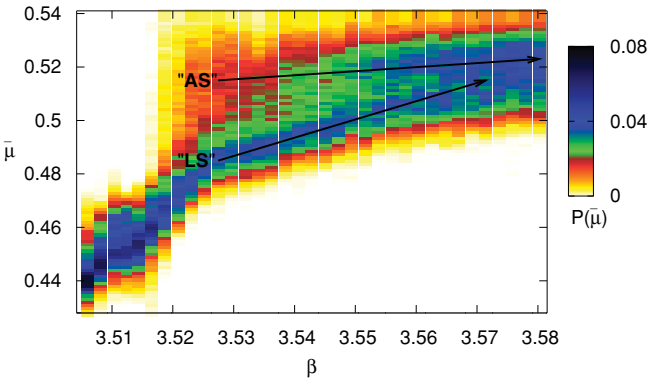

FIG. 4. (Color online) Experimental results showing the combination of histograms for the range of β where AS and LS combine into the mixed state in M and a second Lyapunov exponent emerges in the system. Along with the observation of a smooth transition from low- to high-dimensional dynamics, the multiple peaks (after $\beta \approx 3.55$) indicate UDV existing during the transition. Numerical techniques were also used on the model system to separate and study the individual subsets, and their associated (local) Lyapunov exponents, in isolation (Sec. IV, Fig. 6).

are at greater $\bar{\mu}$ than LS at the same parameter values because AS bifurcated to hyperchaos at lower β than LS and contains more 2D unstable UPOs. This leads to embedded points in the vicinity of AS being more spread into the direction transverse to the synchronization manifold than in LS. Therefore UDV appears strongest while there is mixing between AS and LS, demonstrating the existence of different numbers of bifurcated and unbifurcated UPOs in the combined manifold of the system. The re-absorption of AS into LS can also clearly be seen in this figure. Finally, as AS again dominates, the dimension is seen to tend toward that of a hyperchaotic attractor containing two directions along which trajectories from different initial conditions will diverge. The same types of behavior and transition can also be found in the model system, and investigations using the advanced techniques available to numerical systems are described in Sec. IV.

A. Interaction of the phase synchronized states

In order to fully understand how the two phase states AS and LS interact and combine to form the merged hyperchaotic attractor, the synchronization state in terms of the phase relationship was studied at various parameter values. The phase difference $\Phi = \phi_2 - \phi_1$ between the subsystems 2 and 1 was obtained using the analytic signal method for finite times. Time series of Φ are shown in part (i) of Figs. 5(a)–5(c), with histograms showing the distributions of the density of points as a function of Φ in (ii). In the AS set the phases of O1 and O2 were found to be completely locked, with the phase difference fixed at $\Phi = \pm\pi$. However, in LS the phase difference oscillates in a narrow range of $\Phi \approx 0$ due to the asymmetry of the wave forms, as can be seen in Fig. 5(a). In both AS and LS no phase slips are observed and phase synchronization holds. This is in agreement with there being only a single Lyapunov exponent at zero, indicative of the network acting as a single system. The dynamics of the subsystems suffer phase slips at the merger of AS and LS, separating their dynamics,

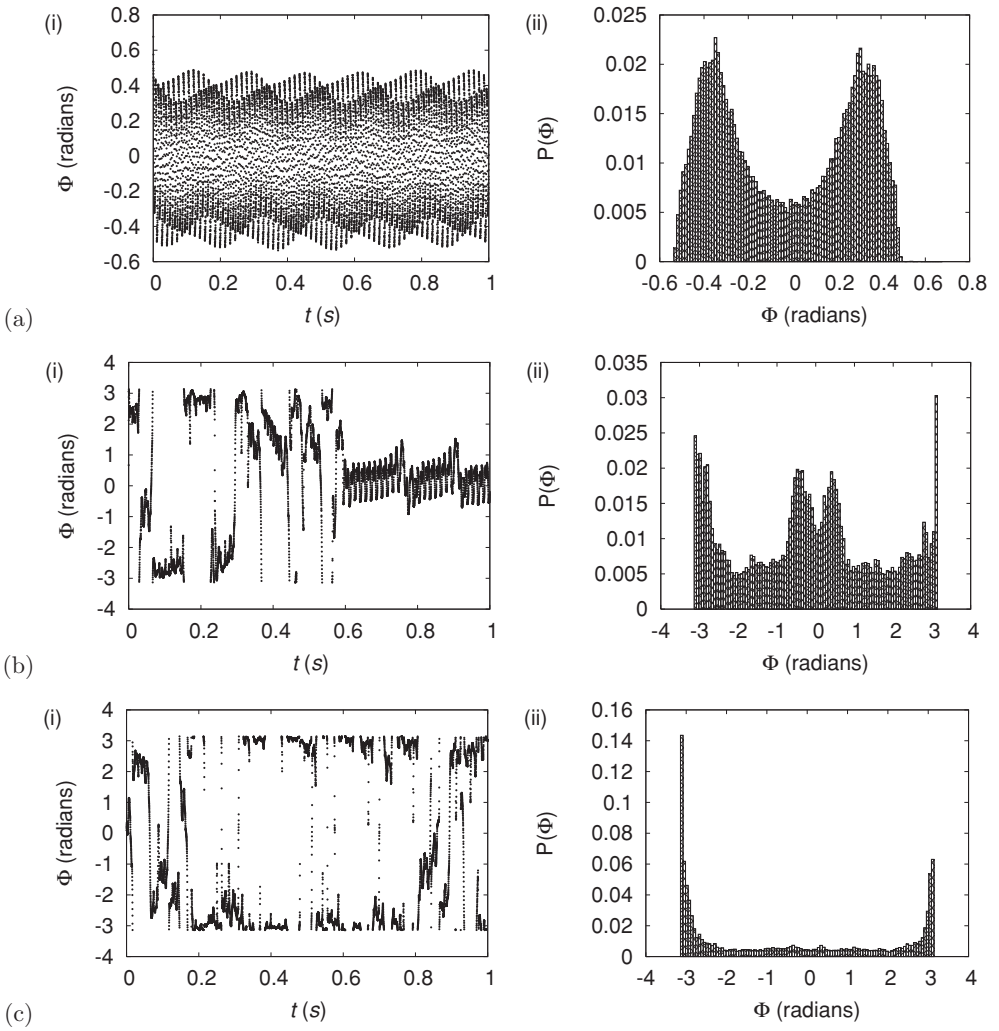

FIG. 5. Phase differences Φ, used for detecting phase synchronization states. At values of β such as shown in (a) ($\beta = 3.356$), where states are in LS, Φ oscillates close to zero. In the M region shown in (b) for ($\beta = 3.532$) intermittencies are found between LS and AS, where $\Phi \approx \pm\pi$ radians. At higher β phases are mainly restricted to $\pm\pi$ radians and trajectories spend most of their time in AS, as shown in (c) ($\beta = 3.602$).

before they again become progressively more unified at higher parameter values. These intermittencies found on the transition between different synchronization regimes can be seen in Fig. 5(b). At such parameter values it was difficult to experimentally measure a Lyapunov exponent at zero, so it is believed that the intermittent loss of phase synchronization in these regimes results in the dynamics of the subsystems temporarily separating from each other. However, as β is further increased trajectories are found to spend less time in LS and the system again approaches phase synchronization, as can be seen in (i) of Fig. 5(c).

IV. NUMERICAL INVESTIGATIONS OF THE STRUCTURE OF THE HYPERCHAOTIC STATE

The equations of motion (2) were used to simulate the system numerically. As well as verifying the experimental results above, the computational techniques used allowed deeper investigation into the structure of the hyperchaotic state. Only a single zero Lyapunov exponent was detected numerically (as well as experimentally) at these higher parameter values, indicating that the system's dynamics, although hyperchaotic, lie on a reduced dimensional manifold. This occurs as phase synchronization is re-established in the system and trajectories spend progressively more time in AS. This demonstrates that, although each of AS and LS develop hyperchaos independently, the final attractor is mainly composed of the hyperchaotic remnant of AS, with a small contribution from LS. Studying the system numerically, the AS and LS states of the attractor were separated using the PIM-simplex method [44]. This makes it possible to isolate unstable saddles contained within the attractor and compute their properties, such as equivalents of their short-time Lyapunov exponents (STLEs). These *local Lyapunov exponents* (LLEs), shown in Fig. 6, are different in magnitude for the two phase states, each originating at different parameter values. The results show that, prior to the loss of stability of LS to the mixed state, each of the positive LLEs of AS is larger than its counterpart in LS, showing a greater degree of instability. However, the rate of increase of the positive LLEs of LS, λ_B, is greater

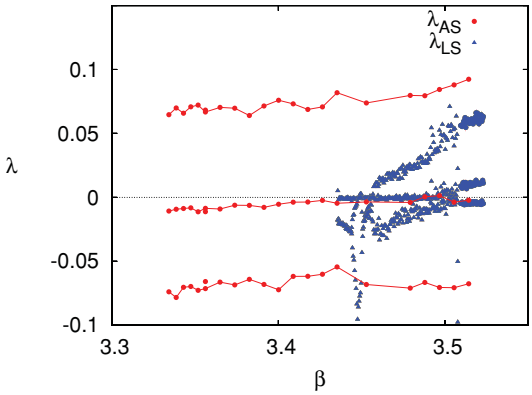

FIG. 6. (Color online) Numerically obtained *local Lyapunov exponents* (LLE—similar to STLEs) for the AS and LS phase states, extending into the unstable parameter regimes for each state. Although AS has greater instability for the studied range (which is constrained by the complexity of the data), the gradient of the LLEs for LS shows that it becomes more unstable at the point where AS becomes dominant in the mixed state. The invariant set became difficult to isolate for parameter values to the right of the diagram and the computing time for the resulting calculations made further extension of the results impossible.

than that for AS, λ_A, and it can be seen that the crossing point can be projected to be approximately at the point where AS becomes dominant in the mixed-phase state. The larger positive LLEs of the LS state and resulting relative instability compared to the AS state explains why AS comes to dominate at higher parameter values and helps complete the picture of the development of high-dimensional *hyperchaotic* dynamics and resulting reduction in predictability.

V. SUMMARY

Understanding the development of hyperchaos and the structure of hyperchaotic attractors is important for knowing the reliability of numerical models through the shadowing theorem, which breaks down in the presence of phenomena such as unstable dimension variability which can be present in hyperchaotic systems. This study has experimentally demonstrated the formation and structure of one type of hyperchaotic attractor and shown many aspects of the transition between synchronized and high-dimensional dynamics in a specific experimental context. Hyperchaos is experimentally observable in this system only after two nonattracting sets have merged. These sets originate in phase-multistable synchronized states, which have differing initial stability due to the induced symmetry in one of the states. These results show clear evidence of a smooth transition to hyperchaos, demonstrating that attractor bubbling, due to the bifurcation of UPOs of the chaotic attractors, is the origin of high-dimensional dynamics in this system. Both sets are therefore believed to develop a second Lyapunov exponent via this route, whereby they become nonattracting hyperchaotic saddles. These eventually combine to form a single merged hyperchaotic attractor, containing within it the remnants of both invariant sets. This is believed to be one possible route to hyperchaos, which may be present in many high-dimensional systems.

ACKNOWLEDGMENTS

We gratefully acknowledge the support of the EPSRC for funding this work, which was carried out in the Manchester Centre for Nonlinear Dynamics at the University of Manchester, UK. We also thank the referees for their specific suggestions for the improvement of this paper.

[1] C. Grebogi, S. M. Hammel, J. A. Yorke, and T. Sauer, Phys. Rev. Lett. **65**, 1527 (1990).
[2] L. M. Pecora and T. L. Caroll, Phys. Rev. Lett. **64**, 821 (1990).
[3] G. S. Duane, J. J. Tribbia, and J. B. Weiss, Nonlinear Proc. Geoph. **13**, 601 (2006).
[4] S. C. Yang, D. Baker, H. Li, K. Cordes, M. Huff, G. Nagpal, E. Okereke, J. Villafañe, E. Kalnay, and G. S. Duane, J. Atmos. Sci. **63**, 2340 (2006).
[5] H. Fujisaka and T. Yamada, Prog. Theor. Phys. **69**, 32 (1983).
[6] A. S. Pikovsky, Z. Phys. B **55**, 149 (1984).
[7] M. G. Rosenblum, A. S. Pikovsky, and J. Kurths, Phys. Rev. Lett. **76**, 1804 (1996).
[8] A. Pikovsky, M. Rosenblum, and J. Kurths, Int. J. Bifurcation Chaos **10**, 2291 (2000).
[9] N. F. Rulkov, M. M. Sushchik, and L. S. Tsimring, Phys. Rev. E **51**, 980 (1995).
[10] G. V. Osipov, B. Hu, C. Zhou, M. V. Ivanchenko, and J. Kurths, Phys. Rev. Lett. **91**, 024101 (2003).
[11] T. Kapitaniak, Y. Maistrenko, and S. Popovych, Phys. Rev. E **62**, 1972 (2000).
[12] I. I. Blekhman, *Synchronization in Science and Technology* (ASME, New York, 1988).
[13] D. E. Postnov, T. E. Vadivasova, O. V. Sosnovtseva, A. G. Balanov, V. S. Anishchenko, and E. Mosekilde, Chaos **9**, 227 (1999).
[14] S. M. Hammel, J. A. Yorke, and C. Grebogi, J. Complex. **3**, 136 (1987).
[15] S. M. Hammel, J. A. Yorke, and C. Grebogi, Bull. Am. Math. Soc. **19**, 465 (1988).
[16] T. Sauer and J. A. Yorke, Nonlinearity **4**, 961 (1991).
[17] Y.-C. Lai, C. Grebogi, J. A. Yorke, and I. Kan, Nonlinearity **6**, 779 (1993).
[18] S. N. Chow and K. J. Palmer, J. Dyn. Diff. Equ. **3**, 361 (1991).
[19] S.-N. Chow and E. S. Van Vleck, SIAM J. Sci. Stat. Comput. **15**, 959 (1994).
[20] Y.-C. Lai, D. Lerner, K. Williams, and C. Grebogi, Phys. Rev. E **60**, 5445 (1999).
[21] S. Dawson, C. Grebogi, T. Sauer, and J. A. Yorke, Phys. Rev. Lett. **73**, 1927 (1994).
[22] T. Sauer, C. Grebogi, and J. A. Yorke, Phys. Rev. Lett. **79**, 59 (1997).
[23] E. J. Kostelich, I. Kan, C. Grebogi, E. Ott, and J. A. Yorke, Physica D **109**, 81 (1997).
[24] Y.-C. Lai and C. Grebogi, Phys. Rev. Lett. **82**, 4803 (1999).
[25] E. Barreto and P. So, Phys. Rev. Lett. **85**, 2490 (2000).

[26] T. Sauer, Phys. Rev. E **65**, 036220 (2002).
[27] N. J. McCullen and P. Moresco, Phys. Rev. E **73**, 046203 (2006).
[28] Silvina Ponce Dawson, Phys. Rev. Lett. **76**, 4348 (1996).
[29] M. A. Harrison and Y.-C. Lai, Phys. Rev. E **59**, 3799 (1999).
[30] R. Davidchack and Y.-C. Lai, Phys. Lett. A **270**, 308 (2000).
[31] F. Takens, *Detecting Strange Attractors in Turbulence*, Lecture Notes in Math. Vol. 898 (Springer, New York, 1981).
[32] H. D. I. Abarbanel, R. Brown, J. J. Sidorowich, and L. Sh. Tsimring, Rev. Mod. Phys. **65**, 1331 (1993).
[33] J. M. Hammersley, Ann. Math. Stat. **21**, 447 (1950).
[34] R. S. Bennett, IEEE Trans. Inf. Theory **IT-15**, 517 (1969).
[35] B. van der Pol, *The Nonlinear Theory of Electric Oscillations*, *Proceedings of the Institute of Radio Engineers*, Vol. 22 (IEEE, 1934), pp. 1051–1086.
[36] J. J. Healey, D. S. Broomhead, K. A. Cliffe, R. Jones, and T. Mullin, Physica D **48**, 332 (1991).
[37] Paul Kerr-Delworth, Ph.D. thesis, University of Manchester, Manchester, UK, 1999.
[38] J. J. Healey, Ph.D. thesis, Oxford University, Oxford, UK, 1991.
[39] J. Abshagen, G. Pfister, and T. Mullin, Phys. Rev. Lett. **87**, 4501 (2001).
[40] H. Haken, J. A. S. Kelso, and H. Bunz, Biol. Cybern. **51**, 347 (1985).
[41] A. Pikovsky, M. Rosenblum, and J. Kurths, *Synchronization (A universal concept in nonlinear sciences)* Cambridge, 2001.
[42] J. W. Swift and K. Wiesenfeld, Phys. Rev. Lett. **52**, 705 (1984).
[43] A. Wolf, J. B. Swift, H. L. Swinney, and J. A. Vastano, Physica D **16**, 285 (1985).
[44] P. Moresco and S. P. Dawson, Physica D **126**, 38 (1999).
[45] G. Benettin, L. Galgani, A. Giorgilli, and J M. Strelcyn, Meccanica **15**, 9 (1980).